An Investigation of the Structural, Connectional, and Functional Subspecialization in the Human Amygdala

Danilo Bzdok,[1,2,3] **Angela R. Laird,**[5,6] **Karl Zilles,**[2,3,4] **Peter T. Fox,**[5,6,7] and **Simon B. Eickhoff**[1,2,3,8]*

[1]*Department of Psychiatry, Psychotherapy, and Psychosomatics, RWTH Aachen University, Aachen, Germany*
[2]*Institute of Neuroscience and Medicine (INM-1), Research Center Jülich, Jülich, Germany*
[3]*Jülich Aachen Research Alliance (JARA)—Translational Brain Medicine, Aachen, Germany*
[4]*C.&O. Vogt Institute of Brain Research, Heinrich Heine University, Düsseldorf, Germany*
[5]*Research Imaging Institute, University of Texas Health Science Center, San Antonio, Texas*
[6]*Department of Radiology, University of Texas Health Science Center, San Antonio, Texas*
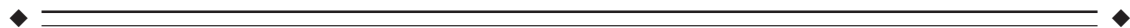[7]*South Texas Veterans Health Care System, San Antonio, Texas*
[8]*Institute of Clinical Neuroscience and Medical Psychology, Heinrich Heine University, Düsseldorf, Germany*

◆━━━━━━━━━━━━━━━━━━━◆

Abstract: Although the amygdala complex is a brain area critical for human behavior, knowledge of its subspecialization is primarily derived from experiments in animals. We here employed methods for large-scale data mining to perform a connectivity-derived parcellation of the human amygdala based on whole-brain coactivation patterns computed for each seed voxel. Voxels within the histologically defined human amygdala were clustered into distinct groups based on their brain-wide coactivation maps. Using this approach, connectivity-based parcellation divided the amygdala into three distinct clusters that are highly consistent with earlier microstructural distinctions. Meta-analytic connectivity modelling then revealed the derived clusters' brain-wide connectivity patterns, while meta-data profiling allowed their functional characterization. These analyses revealed that the amygdala's laterobasal nuclei group was associated with coordinating high-level sensory input, whereas its centromedial nuclei group was linked to mediating attentional, vegetative, and motor responses. The often-neglected superficial nuclei group emerged as particularly sensitive to olfactory and probably social information processing. The results of this model-free approach support the concordance of structural, connectional, and functional organization in the human amygdala and point to the importance of acknowledging the heterogeneity of this region in neuroimaging research. *Hum Brain Mapp 00:000–000, 2012.* © 2012 Wiley Periodicals, Inc.

Key words: amygdala; data mining; parcellation; connectivity; behavior; social cognition

◆━━━━━━━━━━━━━━━━━━━◆

INTRODUCTION

The amygdala has classically been linked to the processing of fearful and unpleasant stimuli [Morris et al., 1996]. Newer evidence, however, extended this concept to the extraction of biological significance from the environment [Sander et al., 2003] and the consequent shaping of behavioral responses [Ousdal et al., 2008]. In line with this view, the amygdala is currently linked to a host of neural processes. This includes classical conditioning [Adolphs, 2008; LeDoux, 2000; Öhman, 2009], social cognition [Adolphs, 2010; Bzdok et al., in press], emotion regulation [Müller et al., 2011; Phelps and LeDoux, 2005], reward processing [Baxter and Murray, 2002], and memory formation [Packard and Cahill, 2001]. Paralleling its functional diversity, the amygdaloid complex has been shown to encompass at least 13 distinct but densely interconnected nuclei in nonhuman primates [Amaral et al., 1992]. Moreover, observer-independent cytoarchitectonic assessment of human postmortem brains allowed the reliable definition of three major sets of nuclei, the so-called laterobasal, centromedial, and superficial groups [Amunts et al., 2005]. Consequently, the prevalent treatment of the amygdaloid complex as a unified entity in neuroimaging studies has been challenged [Swanson and Petrovich, 1998] because its structural features were associated with different functions by research in nonhuman mammals.

Comprehensive studies in rats, cats, and monkeys revealed reasonable homology between the amygdala nuclei regarding microanatomy and connectivity [Price et al., 1987]. Laterobasal, centromedial, and superficial nuclei groups were isolated and thoroughly studied in these three species [McDonald, 1998]. Cytoarchitectonically, the laterobasal nuclei group resembles pyramidal and nonpyramidal neurons of the cerebral cortex [Hall, 1972], while the architecture of the superficial nuclei especially resembles that of the olfactory cortex [McDonald, 1992]. Conversely, the centromedial nuclei group does not resemble the cerebral cortex but shows similarities with cell types in the striatum [Heimer and Van Hoesen, 2006; McDonald, 1992]. Converging evidence established that the laterobasal nuclei group is a site of integration for sensory information, whereas the centromedial nuclei group is a generator of endocrine, autonomic, and somatomotor responses [Davis and Whalen, 2001; LeDoux, 2007; Moreno and Gonzalez, 2007; Pessoa, 2010; Sah et al., 2003]. Concordant with a role in sensory processing, the laterobasal nuclei group was reported to have axonal connections with sensory areas, such as the visual and auditory cortex as well as thalamus, as evidenced by tracing studies in monkeys [Aggleton et al., 1980; Iwai and Yukie, 1987; Yukie, 2002a]. In contrast and concordant with a role in (autonomic) response preparation, the centromedial nuclei group was shown to have axonal connections with the brainstem, hypothalamus, and basal forebrain [Aggleton et al., 1980; Fudge and Haber, 2000; Turner et al., 1980].

In agreement with these observations, functional segregation among amygdalar nuclei has been corroborated by invasive research in living animals. To give an illustrative example in rats, an ibotenic acid lesion study demonstrated a functional double dissociation between the laterobasal and centromedial nuclei group in conditioned fear responses [Killcross et al., 1997]. Animals with laterobasal nuclei lesions were specifically debilitated in choice behavior. Centromedial nuclei lesions, however, led to a selective difficulty in overriding prepotent behavioral responses. In monkeys, single cell recordings found, for instance, that laterobasal neurons in the monkey amygdala responded more selectively to visual stimuli, whereas centromedial neurons responded preferentially to task cues [Mosher et al., 2010]. While the laterobasal and centromedial nuclei groups have thus been well characterized in animals, the superficial nuclei group remains more elusive. Given its connection with the olfactory cortex and the architectonic similarity, the superficial nuclei group appears to relate to the olfactory system [Heimer and Van Hoesen, 2006].

Taken together, previous microscopical investigations, lesion experiments, tracing studies, and single cell recordings in animals provided valuable insight into the structural, connectional, and functional heterogeneity in the amygdala. Consequently, concepts of the amygdala's subspecialization are derived in large part from investigations in animals due to scarce evidence of the connectional and functional heterogeneity in the human amygdala.

Very recent in vivo evidence in humans supports a structural segregation within the amygdala. 7T MRI (magnetic resonance imaging) structural imaging was used to subdivide the amygdala informed by known anatomical features and tissue properties captured by different MRI contrasts [Solano-Castiella et al., 2011]. Additionally, DTI (diffusion tensor imaging) can measure the water mobility in individual seed voxels whose differences were exploited to parcellate the amygdala [Solano-Castiella et al., 2010]. DTI refined by probabilistic tractography locating axonal fiber tracts was able to parcellate the amygdala by differences in anatomical connectivity patters across seed voxels [Bach et al., 2011; Saygin et al., 2011]. In sum, prior noninvasive neuroimaging approaches demonstrated the feasibility of intra-amygdalar compartmentalization in living humans based on tissue properties and white-matter tracts.

In the present study, we investigated the human amygdala's potential subdifferentiation using a data-driven approach. We expected that three different clusters should emerge in the left and right amygdala given three cytoarchitectonically dissimilar subregions in that area [Amunts et al., 2005]. First, each individual seed voxel in the cytoarchitectonically informed volume of interest was submitted to an analysis of its whole-brain coactivation patterns. The seed-voxel-wise coactivation maps were computed by activation likelihood estimation (ALE) meta-analysis over the experiments hosted in the BrainMap database featuring the closest activation foci to the respective seed voxels. Subsequently, these whole-brain

connectivity profiles for each seed voxel were combined into a functional coactivation matrix, representing coactivation likelihood of each seed voxel with each gray-matter voxel. Computing a cross-correlation matrix from this coactivation matrix then provided a quantification of the similarity in whole-brain coactivation profiles between each pair of voxels in the seed volume, i.e., the histologically defined amygdala. Groups of seed voxels featuring similar connectional profiles were then identified by a spectral reordering approach, which was cross-validated against hierarchical clustering as well as against nonhierarchical k-means clustering. The ensuing connectivity-derived clusters were subsequently submitted to cytoarchitectonic assessment. Second, brain-wide coactivation maps were generated for the derived intra-amygdalar clusters to delineate their task-based functional connectivity patterns. Third, the clusters identified within the human amygdala were functionally characterized by assessing the neuroimaging tasks activating the respective regions. In a hypothesis-free manner, we thus investigated structural, connectional, and functional properties of subregions in the human amygdala.

METHODS

Data Used for the Neuroinformatic Analysis

Our volume of interest (VOI) was derived from a histological definition of the amygdala using the SPM Anatomy Toolbox [Eickhoff et al., 2005, 2006]. In particular, the bilateral amygdala has previously been cytoarchitectonically mapped in 10 human postmortem brains, 3D reconstructed, and registered to MNI space [Montreal Neurological Institute; Amunts et al., 2005; Zilles et al., 2002]. The resulting "maximum probability map" (MPM) holds the occurrence likelihood of cortical fields at each brain voxel. This MPM thus provides a continuous, nonoverlapping representation of microanatomically defined brain areas. Given its representation of histological data in standard space, the seed region for the current analysis was defined by the MPM representation of the human amygdala. This allowed including only those voxels into the VOI where the amygdala had been more likely found than any other brain region in histological examination (Fig. 1). It should be noted that normalization into standard space as well as representation of microscopical structures in $2 \times 2 \times 2$ mm^3 voxel space may entail a slightly liberal definition of the human amygdala. This is because each voxel may not correspond precisely to histologically defined amygdala tissue at micrometer resolution. Nevertheless, we would regard the MPM-based definition of the amygdala seed region as the biologically most valid representation of the amygdala in standard space, with currently no available alternative based on in vivo imaging. The VOI was submitted to a model-free parcellation that grouped seed voxels based on similarities between coactivation patterns of the individual seed voxels [Eickhoff et al., 2011] across
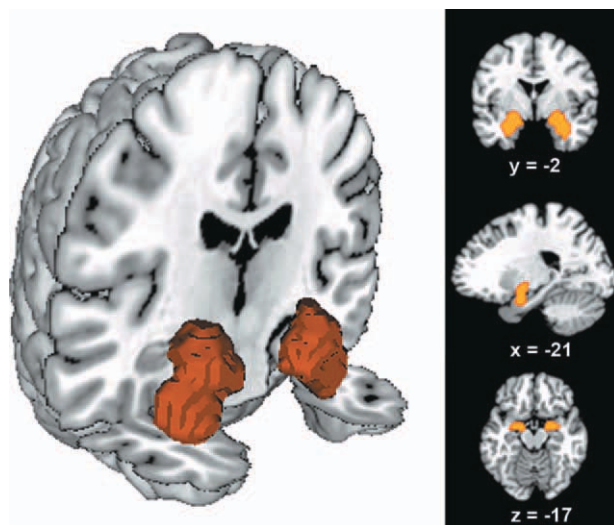

Figure 1.

Location of the volume of interest. The seed region was based on probabilistic maps of the amygdala obtained from the Jülich histological atlas [Amunts et al., 2005]. The left image was rendered using Mango (multi-image analysis GUI; http://ric.uthscsa.edu/mango/). Renderings in right column depict coronal, sagittal, and axial sections through the seed region rendered into a T1 weighted MNI single subject template.

neuroimaging experiments archived in the BrainMap database [Fox and Lancaster, 2002].

Meta-analytic Connectivity Mapping

Delineation of whole-brain coactivation maps for each individual seed voxel was performed based on the BrainMap database [www.brainmap.org; Fox and Lancaster, 2002; Laird et al., 2011]. We constrained our analysis to databased functional magnetic resonance imaging (fMRI) and positron emission tomography (PET) experiments from normal neuroimaging studies (no interventions, no group comparisons) in healthy subjects that report results as coordinates in stereotaxic space. These inclusion criteria yielded ~6,500 eligible functional neuroimaging experiments at the time of analysis. Note that we considered all eligible BrainMap experiments because any preselection of taxonomic categories would have constituted a fairly strong a priori hypothesis about how brain networks are organized. Yet, it remains elusive how well psychological constructs, such as emotion and cognition, map on regional brain responses [Laird et al., 2009a; Poldrack, 2006].

To reliably determine the coactivation patterns of a given seed voxel, we identified the set of experiments in BrainMap that reported closest activation to that voxel. This was achieved by calculating the respective Euclidean distances between the current seed voxel and the individual foci of all databased experiments. That is, the experiments associated with each seed voxel were defined by

activation at or in the immediate vicinity of this particular seed voxel. The brain-wide coactivation pattern for each seed voxel was then computed by quantitative meta-analysis over the hereby associated experiments [Eickhoff and Bzdok, 2012].

A challenge in constructing coactivation maps is the limited number of experiments activating precisely at a particular seed voxel and the lack of any objective measure how many closest experiments should be considered when computing coactivation. We therefore systematically analyzed a broad range of sets of associated experiments to increase the robustness of our parcellation and to avoid dependence on any particular user-specified parameter, such as the specific number of included experiments. More precisely, we computed 14 MACM (meta-analytic connectivity modeling) coactivation maps for every single seed voxel by moving from employing the closest 25 up to closest 90 associated experiments in steps of five (i.e., closest 25, 30, 35..., 90 experiments) for this particular voxel. The ensuing 14 preliminary coactivation maps of each seed voxel were then merged into one final coactivation map per seed voxel by computing their voxel-wise median. We thus generated a highly robust coactivation map for every seed voxel that should not depend on user-defined choices about the number of associated experiments and hence provided a reliable basis for connectivity-based parcellation.

As noted, the key rationale behind using experiments in the close vicinity of a particular seed voxel is to provide a more robust computation of coactivation patterns given the limited number of experiments activating precisely at each voxel. It is noteworthy that the actual spatial dispersion, i.e., induced smoothness, is very small. In particular, the mean distance of the foci, whose experiments were included in the computation of the coactivation map, ranged from 3.24 mm (closest 25 experiments) to 5.18 mm (closest 90 experiments), i.e., from 1.6 to 2.6 voxels. This confirms that, indeed, only BrainMap experiments activating in the immediate neighborhood of the respective seed voxel contributed to the MACM connectivity analyses.
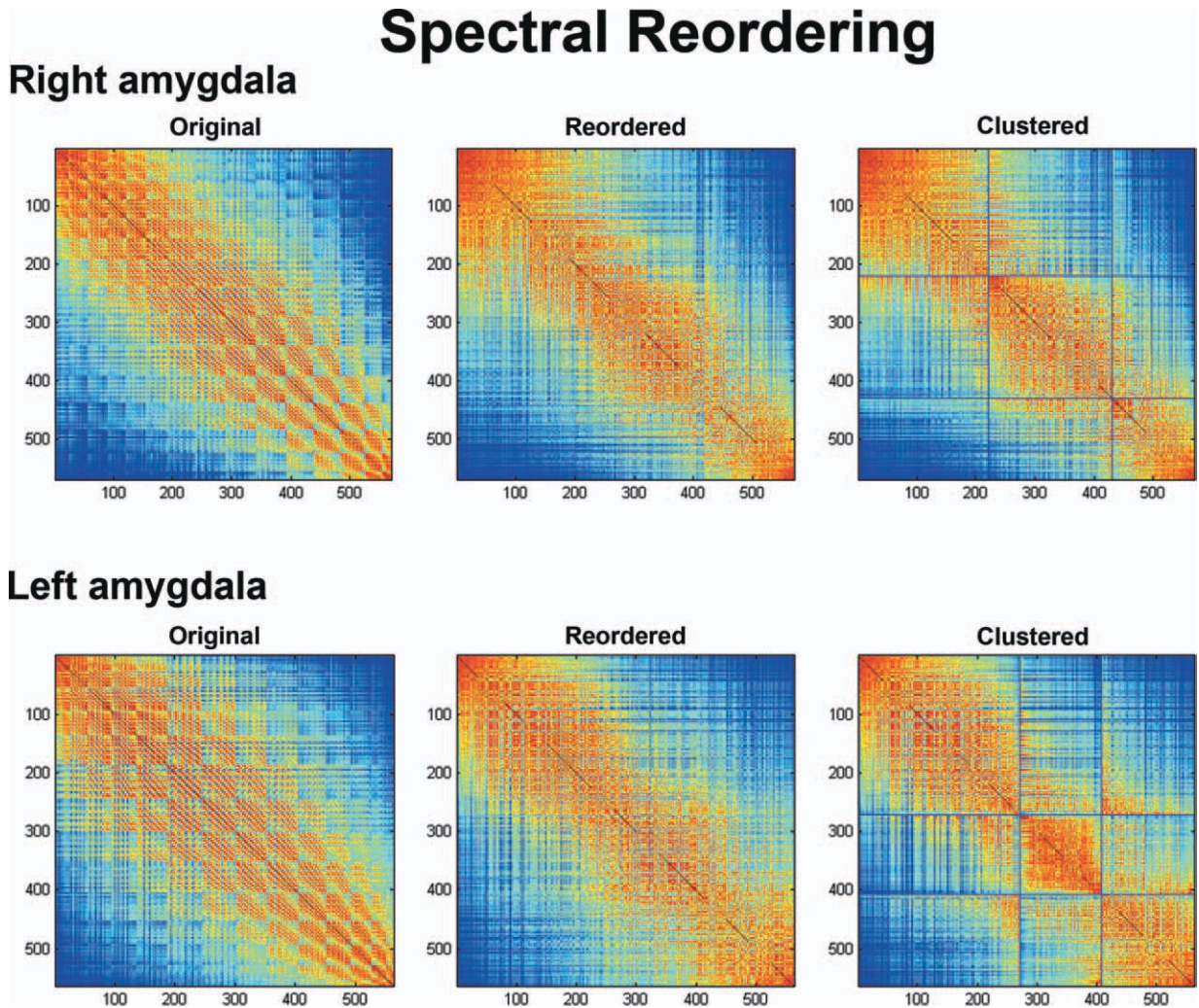
The brain-wide coactivation pattern for each individual seed voxel was then computed by activation likelihood estimation (ALE) meta-analysis over the experiments that were associated with that particular voxel by the procedure outlined above [Eickhoff et al., 2009; Laird et al., 2009a; Turkeltaub et al., 2002]. The key idea behind ALE is to treat the foci reported in the associated experiments not as single points, but as centers for 3D Gaussian probability distributions that reflect the spatial uncertainty associated with neuroimaging results. As we used the most up-to-date ALE implementation [Eickhoff and Bzdok, in press; Eickhoff et al., in press], the spatial extent of those Gaussian probability distributions was based on objective empirical estimates of between-subject and between-template variance of neuroimaging foci [Eickhoff et al., 2009]. For each experiment, the probability distribution of all reported foci were then combined into a modeled activation (MA) map by the recently introduced "nonadditive" approach that prevents local summation effects [Turkeltaub et al., 2011]. We employed the more precise analytical solution for statistical inference, which moreover allows cluster-level thresholding [Eickhoff et al., in press]. The voxel-wise union across the MA maps of all experiments associated with a particular seed voxel then yielded an ALE score for each voxel of the brain that describes the coactivation probability of that particular location with the current seed voxel. The ALE scores of all voxels within the gray-matter (based on 10% probability according to the ICBM [International Consortium on Brain Mapping] tissue probability maps) were then recorded before moving to the next voxel of the seed region.

Taken together, quantitative meta-analysis over all foci reported in the experiments associated with the current seed voxel determined how likely any other voxel throughout the brain was to coactivate with that particular seed voxel. Note that no threshold was applied to the ensuing coactivation maps at this point of analysis to retain the complete pattern of coactivation likelihood. These coactivation maps actually reflect functional connectivity between the seed region and the rest of the brain as this approach rests on the "temporal correlation of spatially distant neurophysiological events" [Friston et al., 1996].

Connectivity-Based Parcellation: Structural Parcellation Based on Coactivation Patterns

The unthresholded brain-wide coactivation profiles for all seed voxels were subsequently combined into a $N_S \times N_B$ coactivation matrix, where N_S denotes the number of seed voxels (563 in left amygdala, 569 in the right amygdala) and N_B the number of voxels in the reference brain volume at $2 \times 2 \times 2$ mm^3 resolution (~260,000 voxels located within gray-matter). Importantly, we computed not one but several different coactivation maps corresponding to each seed voxel using a variety of associativity measures (see above). This set of preliminary coactivation maps of each seed voxel now allowed averaging those into a single final coactivation map to base subsequent analysis on robust connectivity of every seed voxel. In particular, sets of voxels that feature similar brain-wide coactivation profiles were grouped by hierarchical cluster analysis [Eickhoff et al., 2007; Timm, 2002]. In this approach, individual voxels initially form separate clusters which are then successively included into a hierarchy merging the least dissimilar clusters to derive progressively larger clusters of voxels. Correlation between the brain-wide coactivation profiles of seed voxels was used as a similarity measure and average linkage criterion for cluster merging [Timm, 2002]. In sum, the seed voxels were thus merged as a function of correspondence of their coactivation profiles to subdivide the VOI into clusters of convergent functional connectivity.

Spectral Reordering

Figure 2.

Original, reordered, and clustered connectivity cross-correlation matrices. Cross-correlations between coactivation patterns of individual seed voxels (563 in left amygdala, 569 in the right amygdala). Three sets of voxels that feature similar brain-wide coactivation profiles emerged in the reordered cross-correlation matrix and were subsequently grouped by hierarchical cluster analysis.

The most appropriate number of clusters in the left and right amygdala was determined by a $N_S \times N_S$ cross-correlation matrix, analogous to previous connectivity-based parcellation approaches [Johansen-Berg et al., 2004; Kim et al., 2010]. This matrix reflected a symmetric summary of how strongly seed voxels' connectivity profiles correlated with each other (cf. Fig. 2). The matrix was then reordered to minimize the cross-correlation values off the diagonal, hereby forcing closely correlated voxels close to each other. In doing so, sets of seed voxels emerged that were strongly correlated with each other and weakly correlated with the rest of the matrix. It was this reordered correla-

tion matrix that favored parcellation into specific number of clusters.

Characterization of the Connectivity-Derived Clusters: Coactivations

Following the connectivity-based parcellation of the seed region into separate clusters, another MACM analysis was performed on each of the ensuing clusters to characterize their coactivation patterns. In this context, "clusters" refers to sets of voxels within the seed region that were

identified by the coactivation-based parcellation outlined above as having similar coactivation patterns to each other but distinct to the rest of the seed voxels. Please note that the above MACM analysis assessed seed-voxel-wise connectivity patterns to obtain each seed voxels' individual functional-connectional properties, while we here assessed the overall connectivity pattern of a set of seed voxels, namely, the individual connectivity-derived clusters. Additionally, the above MACM analysis considered BrainMap experiments close to individual seed-voxels, while we here considered all BrainMap experiments featuring at least one focus of activation within the cluster. Then, ALE meta-analysis was performed on the obtained pool of selected experiments as described above. Statistical inference was additionally sought in contrast to the MACM analysis underlying connectivity-based parcellation. That is, to establish which regions were significantly coactivated with a particular cluster of voxels, ALE scores for the MACM analysis of this cluster were compared to a null-distribution that reflects a random spatial association between experiments, but regards the within-experiment distribution of foci as fixed [Eickhoff et al., 2009]. This random-effects inference assesses above-chance convergence between experiments, not clustering of foci within a particular experiment. The observed ALE scores from the actual meta-analysis of experiments activating within a particular cluster were then tested against the ALE scores obtained under this null-distribution yielding a P value based on the proportion of equal or higher random values. The resulting P values were then thresholded at a cluster-level family-wise error (FWE) corrected threshold of $P < 0.05$.

Overlap between the brain-wide coactivation patterns of the connectivity-derived clusters was identified using a minimum-statistic conjunction, i.e., by computing the intersection of the thresholded ALE-maps [cf. Bzdok et al., in press]. Differences in coactivation patterns between two connectivity-derived clusters were assessed by first performing MACM separately on the experiments associated with either cluster and computing the voxel-wise difference between the ensuing ALE maps [Eickhoff et al., 2011]. All experiments contributing to either analysis were then pooled and randomly divided into two groups of the same size as the original two sets of experiments (corresponding to those activating in either cluster). ALE-scores for these two randomly assembled groups were calculated and the difference between these ALE-scores was recorded for each voxel in the brain. Repeating this process 10,000 times then yielded a null-distribution in ALE-scores between the MACM analyses of the two clusters. The observed difference in ALE scores was then tested against this null-distribution yielding a P value for the difference at each voxel based on the proportion of equal or higher random differences. The resulting nonparametric P values were thresholded at $P < 0.001$.

Of note, BrainMap experiments built the basis for both coactivation-based parcellation and subsequent connectivity analysis of the emerging clusters. This does, however, not imply circular reasoning. Rather, delineation of the coactivation patterns of the obtained clusters illustrates and further characterizes the regional connectional heterogeneity that actually led to cluster formation. Consequently, the analysis of brain-wide coactivation maps for the ensuing clusters represents an important follow-up analysis that permits to appreciate the coactivation patterns underlying the clustering process.

Characterization of the Connectivity-Derived Clusters: Function

The functional characterization of the coactivation-derived clusters was based on the BrainMap meta-data that describes the specific mental processes isolated by the archived experiments' statistical contrasts [Fox et al., 2005]. Behavioral domains (BD) comprise the main categories cognition, action, perception, emotion, and interoception, as well as their related subcategories. Paradigm classes (PC) categorize the specific task employed (see http://brainmap.org/scribe/ for a complete list of BDs and PCs). We analyzed the behavioral domain and paradigm class meta-data of databased experiments associated with each identified cluster to assess the distribution of domain "hits" relative to the entire database. In particular, functional profiles of the derived clusters were determined by significant overrepresentation of BDs and PCs in the experiments activating a particular cluster relative to the BrainMap database using a binomial test [$P < 0.05$, corrected for multiple comparisions using Bonferroni's method; Eickhoff et al., 2011; Laird et al., 2009b; Nickl-Jockschat et al., 2011].

Please note that the BrainMap taxonomy resulted from 20 years of continuous refinement [Laird et al., 2009c]. The accuracy and consistency of every single database entry is ensured by BrainMap staff and cross-checked by faculty. Moreover, there is a generally recognized lack of a widely accepted ontology of cognitive processes [Poldrack, 2006; Price and Friston, 2005; Toga, 2002]. As a consequence, we deem the functional characterization of the connectivity-derived clusters informative, as BrainMap provides one of the currently best described and validated taxonomies.

RESULTS

In line with histological properties of the amygdala in human postmortem brains [Amunts et al., 2005], the present connectivity-based parcellation (CBP) indicated a separation into three clusters of seed voxels. Those seed voxel sets demonstrated very high within-cluster and very low between-cluster correlation in a spectral reordering approach (Fig. 2). The emerged three-cluster-solution was subsequently cross-validated by high consistency across
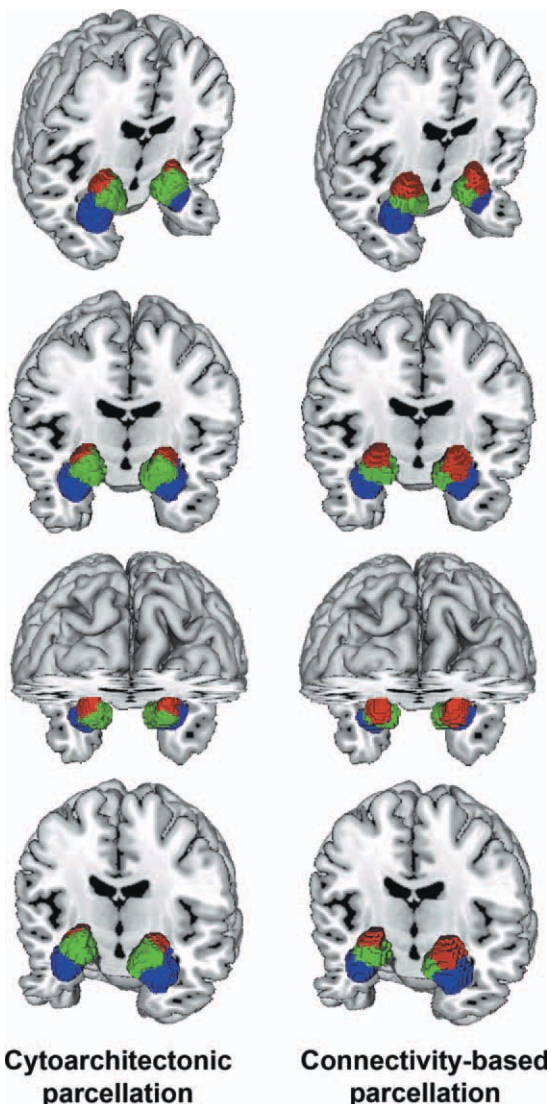
cordantly shaped in both hemispheres. Third, exploratory parcellation into more than three clusters yielded contradictory results across hemispheres (Supporting Information Fig. S2).

Consistency of the Parcellation Pattern Across Diverging Grouping Procedures

We employed the spectral reordering approach as previously established for connectivity-based parcellation using DTI and resting-state data [Johansen-Berg et al., 2004; Kim et al., 2010]. Of note, this approach differs from the hierarchical clustering or the, now also employed, *k*-means clustering by primarily providing a representation of the data (cross-correlation matrix) that allows visually identifying the number of distinct components within it. When examining the spectrally reordered cross-correlation matrix for our VOI, it revealed a rather distinct subdivision into three groups of voxels. In particular, these three sets of seed voxels were strongly correlated with each other and weakly correlated with the rest of the matrix. In contrast to the other approaches, it should be stressed that spectral reordering does not depend on any choices regarding parameters and association measures. This representational approach thus provided evidence for the presence of three distinct clusters in a bottom-up fashion.

In addition to spectral reordering, we performed hierarchical cluster analysis as a function of similarity between the seed voxels' connectional fingerprints. Hierarchical clustering is a multivariate method for solving classification problems by revealing similarities and dissimilarities between elements in a multidimensional feature space. More specifically, individual voxels initially formed separate clusters which were then successively included into a hierarchy merging the least dissimilar clusters to derive progressively larger clusters of voxels. This analysis yielded the three clusters reported and discussed in this article. As a result of the review process, we also investigated a potential parcellation of our seed region using the nonhierarchical *k*-means clustering algorithm. *K*-means clustering is an iterative algorithm that can be used to divide a seed region into a preselected number of *k* clusters [Hartigan and Wong, 1979]. Given that the ensuing clusters can vary with the starting point that needs to be chosen initially, the algorithm is usually repeated numerous times [Nanetti et al., 2009]. We repeated *k*-means clustering 1,000 times and recorded the most optimal solution, i.e., the assignment yielding the global minimum of the cost-function. Importantly, we performed both hierarchical and *k*-means clustering on the very same cross-correlation matrix to compare the parcellation schemes revealed by these two fundamentally different clustering approaches.

We would argue that convergence of the individual parcellations obtained from both approaches up to a certain number of clusters would provide a strong data-driven argument for the respective solution. In particular, a

Figure 3.

Renderings of cytoarchitectonic versus connectivity-derived parcellation. Connectivity-derived clusters on the right show spatial continuity and localization in accordance with microscopically observed clusters on the left [Amunts et al., 2005]. Blue = corresponds to laterobasal nuclei group, red = corresponds to centromedial nuclei group, green = corresponds to superficial nuclei group. Images were rendered using Mango.

hierarchical and *k*-means clustering (see below). Three pieces of evidence further attested to the robustness and biological meaningfulness of the three-cluster solution. First, the derived clusters were spatially continuous (Fig. 3). That is, each cluster consisted of a single, identically classified volume without "enclaves" of voxels that would represent minority assignments comparing to their neighboring voxels. Second, the derived clusters were con-

TABLE I. Quantitative overlap between cytoarchitecture and connectivity-based parcellations of the human amygdala

	Left amygdala			Right amygdala		
	cluster 1	cluster 2	cluster 3	cluster 1	cluster 2	cluster 3
cluster overlap with LB	33%	5%	**96%**	16%	39%	**98%**
cluster overlap with CM	**38%**	0%	0%	**56%**	0%	0%
cluster overlap with SF	28%	**94%**	3%	27%	**60%**	0%
LB overlap with cluster	17%	2%	**68%**	4%	23%	**62%**
CM overlap with cluster	**81%**	0%	0%	**85%**	1%	0%
SF overlap with cluster	31%	**53%**	4%	15%	**66%**	0%
→ cluster identified as	CM	SF	LB	CM	SF	LB

Using the SPM Anatomy Toolbox (Eickhoff et al., 2005), we tested whether the connectivity derived clusters topographically correspond to microanatomically defined cytoarchitectonic sub-regions (i.e., MPMs, maximum probability maps) of the amygdala (Amunts et al., 2005), individually in each hemisphere. The upper three rows indicate the extent to which the clusters overlapped with the MPM representations. Conversely, the lower three rows indicate the extent to which the MPM representations overlapped with the clusters. This analysis revealed that the computationally derived clusters map onto histologically distinct nuclei in the amygdala. LB = laterobasal nuclei group, CM = centromedial nuclei group, SF = superficial nuclei group.

strong argument for the three-cluster solution could be provided if the assignment of the seed voxels to three clusters is consistent between hierarchical and *k*-means clustering, while the assignment into four clusters is inconsistent. This was indeed the outcome we observed when comparing both approaches for the 14 cross-correlation matrices (MACM on the 25 to 90 closest BrainMap experiments—in steps of 5).

Cytoarchitectonic Assignment of the Connectivity-Derived Clusters

After the identification of three distinct connectivity-based clusters in the VOI, we tested the hypothesis that these might correspond to microscopically distinct nuclei. To this end, the three connectivity-derived clusters in the left and right amygdala were anatomically assigned according to cytoarchitectonic probability maps of the human amygdala [Amunts et al., 2005] using the SPM Anatomy toolbox [Eickhoff et al., 2006]. In the left amygdala, cluster 1 coincided with 81% of the volume that was histologically specified as centromedial nuclei group. About 94% of cluster 2 was assigned to the superficial nuclei group and 96% of cluster 3 was assigned to the laterobasal nuclei group. In the right amygdala, cluster 1 coincided with 85% of the histologically defined centromedial nuclei group, 60% of cluster 2 was assigned to the superficial nuclei group, and 98% of cluster 3 was assigned to the laterobasal nuclei group. Please note that, above, "assigned to" refers to the extent to which a given cluster overlapped with a given MPM representation. Conversely, "coincided with" refers to the extent to which a given MPM representation overlapped with a given cluster. This distinction essentially expresses the intersection volume as a percentage of the cluster volume or as a percentage of the MPM representation, respectively. Please see Table I for a detailed list of overlap assessments.

That is, we report a high concordance of the three computationally derived clusters in each hemisphere with the cytoarchitectonic definitions of the centromedial (CM), superficial (SF), and laterobasal (LB) nuclei groups that comprise the amygdala [Amunts et al., 2005]. Taken together, without a priori constraints imposed on our investigation, cluster formation driven by dissimilarity in coactivation patterns distinguished three subregions in the seed VOI. Those subregions map well onto the three microanatomically defined subregions of the amygdala [Amunts et al., 2005]. This was revealed by a comparison of the CBP results with the histological maximum probability map in MNI space (Fig. 3).

Interhemispheric Correspondence

Intriguingly, three clusters were established as optimal solution separately in each hemisphere. In particular, the existence of three clusters was indicated by individual spectral reorderings pertaining to the left and right amygdala without any particular a priori hypothesis. Moreover, hierarchical and *k*-means clustering provided converging results only up to this solution. A post-hoc cytoarchitectonic assessment of the emerged parcellation schemes revealed very good correspondence with microstructurally defined subregions in the left and right amygdala.

The observed symmetry of amygdalar organization across hemispheres might be surprising in light of prior evidence suggesting functional and connectional asymmetry. For instance, in rats, left amygdala kindling decreased anxiety for at least 1 week, whereas right amygdala
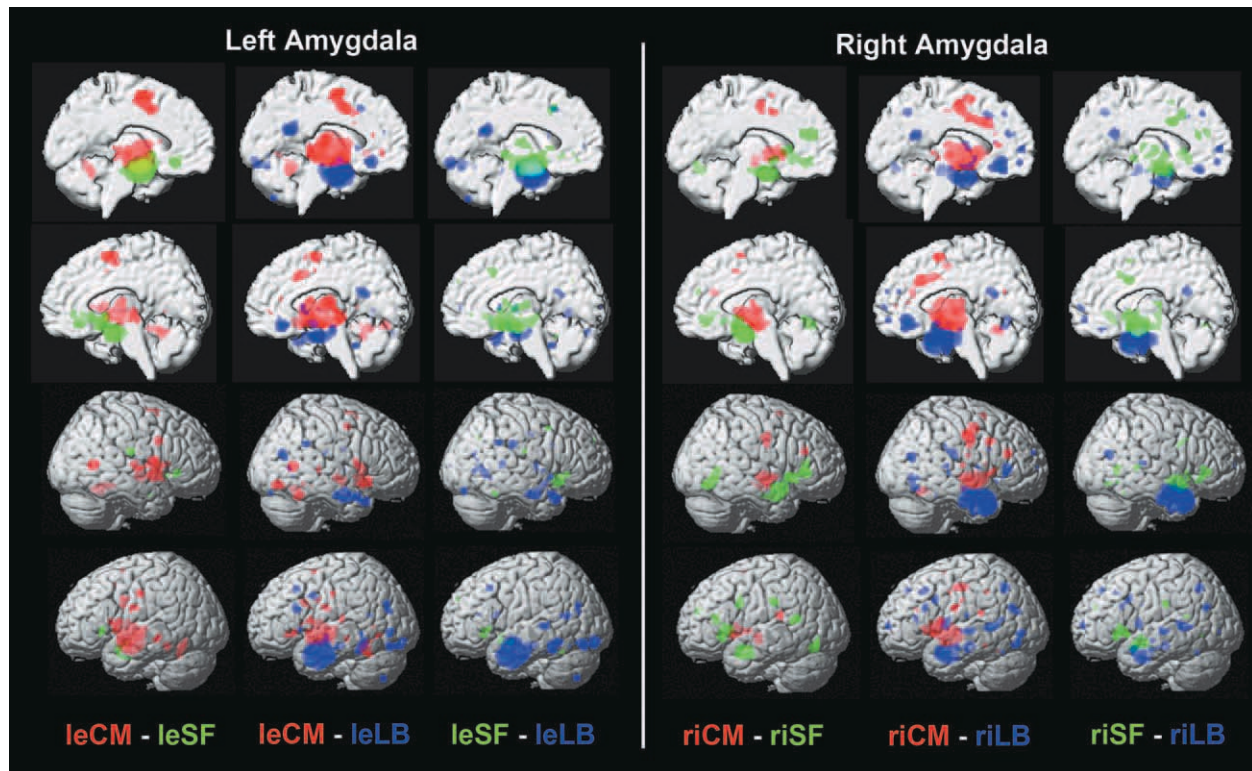
Figure 4.

Difference analyses between coactivation maps of the derived clusters. Difference analyses between the coactivation maps of any combination of two clusters, separately in each hemisphere, to quantify how individual clusters' coactivation maps relate to each other. For each pair of the three delineated clusters (one pair per column), we performed the following procedure. First, each cluster's connectivity map was computed using MACM (cf., Supporting Information Fig. 1). Second, the difference analysis on each pair of connectivity maps yielded voxels that were significantly more likely coactivated with either cluster (cf. Method section). Column-wise, the clusters and corresponding coactivations are color coded. Rendered on T1 MNI single subject template. le = left, ri = right, LB = laterobasal nuclei group, CM = centromedial nuclei group, SF = superficial nuclei group.

kindling increased anxiety [Adamec and Morgan, 1994]. Furthermore, an fMRI study in humans showed increased connectivity between the right amygdala, pulvinar, and superior colliculus using masked versus nonmasked fear-conditioned faces, which was not observed in the left amygdala [Morris et al., 1999]. In another fMRI study the left, but not right, human amygdala distinguished changes in the eye region associated with fear versus gaze [Hardee et al., 2008]. In sum, the topographically symmetric subregions in the left and right amygdala, obtained in this study, seem to be characterized by partly asymmetric connectional and functional properties as evidenced by earlier research.

Coactivation Patterns of the Connectivity-Derived Clusters

Following anatomical assignment, each derived cluster's coactivation map was determined by ALE meta-analysis across all BrainMap experiments activating that region

(i.e., MACM). Those task-based coactivation maps, reflecting the functional connectivity of each cluster in the left and right amygdala, were then family-wise error corrected at $P < 0.05$ (Supporting Information Fig. S1). Interestingly, the three clusters share a marked amount of common connectivity, while their distinctness is significant in enabling parcellation in the first place. Subsequently, we conducted difference analyses between the coactivation maps of any combination of two clusters, separately in each hemisphere, to interrogate how individual clusters' coactivation maps relate to each other (Fig. 4). To, however, isolate the brain areas that were most selectively connected with a given cluster, we parceled out that clusters' functional connectivity shared with the respective two other clusters. For example, to delineate coactivation exclusive to cluster 1, we computed an AND conjunction between the two difference maps (cluster 1–cluster 2) and (cluster 1–cluster 3), thereby effectively removing connectivity shared with cluster 2 and 3. An extent threshold of $k = 10$ voxels was applied to the ensuing coactivation maps.

The left cluster identified as laterobasal nuclei group (332 associated neuroimaging experiments) was selectively coactivated with the precuneus, inferior occipital gyrus, cerebellum, superior temporal gyrus/associative auditory cortex, and middle frontal gyrus/frontal eye field on the left side, as well as bilateral temporal pole and right inferior parietal cortex (Fig. 5). The right cluster identified as laterobasal nuclei group (277 associated neuroimaging experiments) was selectively coactivated with the dorsomedial prefrontal cortex, temporal pole, precuneus, and inferior parietal cortex bilaterally, as well as the ventromedial prefrontal cortex, superior temporal gyrus/associative auditory cortex, middle frontal gyrus/frontal eye field, hippocampus, and posterior superior temporal sulcus on the left side. In sum, the LB clusters were connected with earlier visual cortices as well as various associative sensory brain areas known to process higher-level visual and auditory input. Additionally, especially the right LB clusters selectively coactivated with medial prefrontal cortex, inferior parietal cortex, and precuneus, collectively referred to as the "default mode network" [Buckner et al., 2008].

The left cluster identified as centromedial nuclei group (442 associated neuroimaging experiments) was connected to the supplementary motor cortex (BA 6), pallidum, putamen, cerebellum, insula, and thalamus bilaterally (Fig. 5; activation in right pallidum/putamen and bilateral cerebellum is not depicted), as well as left posterior mid-cingulate cortex, left primary somatosensory cortex (BA 3), and right occipital lobe (V5). The right cluster identified as centromedial nuclei group (331 associated neuroimaging experiments) was connected to the primary motor cortex (BA 4), supplementary motor cortex (BA 6), pallidum, putamen, primary somatosensory cortex (BA3), and inferior frontal gyrus bilaterally, as well as the right thalamus and left insula. In sum, the CM clusters were connected to brain areas implicated in motor behavior, perceptual modulation, as well as visceral and somatosensory processing.

Finally, the left cluster identified as superficial nuclei group (273 associated neuroimaging experiments) was selectively coactivated with the ventral striatum/nucleus accumbens and olfactory tubercle bilaterally, as well as with the right anterior insula (Fig. 5). The right cluster identified as superficial nuclei group (373 associated neuroimaging experiments) was selectively connected to the left anterior mid-cingulate cortex and bilateral anterior insula, extending into the inferior frontal gyrus. In fact, the SF clusters coactivated a slightly more rostral part of the anterior insula compared to the CM clusters. In sum, the SF clusters were connected to brain areas involved in reward prediction, olfaction as well as affective and vegetative processing.

Consistency of Results Across VOIs and CBP Implementations

In a supplementary analysis, we addressed the possible concern that the observed parcellation of the amygdala could have been driven by neighboring brain structures, rather than connectional differences throughout the actual amygdala tissue. We thus recomputed CBP of the cytoarchitectonic seed region from the Jülich atlas while restricting seed-voxel-wise MACM analysis to BrainMap experiments activating strictly within brain regions that were cytoarchitectonically assigned to the amygdala. Importantly, on average 92% of the seed voxels in the left and right amygdala were assigned to the same clusters as in the main analysis (left CM: 91%, left SF 94%, left LB 96%, right CM 96%, right SF 82%, right LB 94%; Fig. 6, left versus middle column). Moreover, a highly similar parcellation pattern was observed using the same anatomically constrained CBP analysis in an unrelated, spatially much more restricted macroanatomical amygdala seed region (Fig. 6, right column) drawn from the probabilistic Harvard-Oxford atlas distributed with the FSL software package [http://www.fmrib.ox.ac.uk/fsl/fslview/atlas-descriptions.html#ho; Smith et al., 2004]. We thus observed converging evidence for the coactivation-based parcellation of the amygdala across two diverging CBP implementations (choosing the nearest voxels without further constraints and constraining the analysis to voxels within the histologically identified amygdala) and two independent seed regions (Jülich cytoarchitectonic atlas versus Harvard-Oxford macroanatomical atlas).

After this cross-validation of the obtained parcellation scheme, we also performed additional connectivity analyses for the amydala clusters obtained from the more conservative, anatomically constrained CBP approach of the histological seed region. Analogous to the main analysis, coactivation patterns of individual clusters were initially revealed by MACM (Supporting Information Fig. S6). This time, however, we restricted the analysis to BrainMap experiments activating within the histologically identified amygdala. Functional connectivity specific to a given clusters was then determined by computing a conjunction (Supporting Information Fig. S8) between the difference analyses (Supporting Information Fig. S7) of coactivation maps with the respective two other clusters. In agreement with the initial analysis, the clusters corresponding to LB were connected with the visual and auditory cortex, posterior superior temporal gyrus, middle frontal gyrus, ventro/dorsomedial prefrontal cortex, temporal pole, inferior occipital gyrus, precuneus, hippocampus, and cerebellum. The clusters corresponding to CM were consistently connected to the insula, inferior frontal gyrus, supplementary motor area/posterior mid-cingulate cortex, thalamus, primary motor cortex, basal ganglia, cerebellum, and somatosensory cortex. MT/V5, however, was not revealed in this additional analysis. Finally, the clusters corresponding to SF were consistently connected to the ventral striatum/nucleus accumbens, olfactory tubercle, and anterior insula/inferior frontal gyrus, yet, did not relate to the anterior mid-cingulate cortex. In line with the converging evidence from the
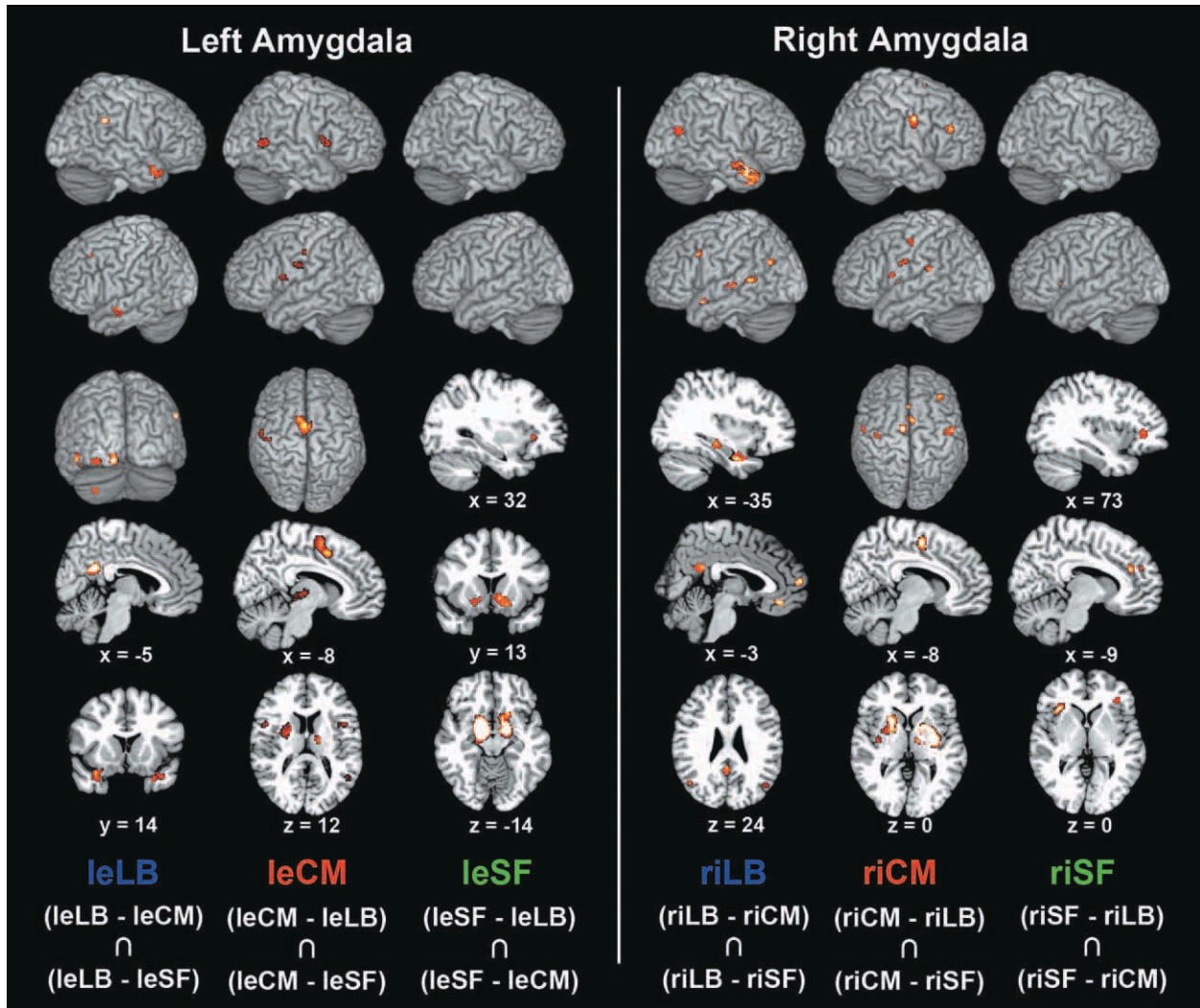
Figure 5.

Connectivity patterns specific to individual derived clusters in the left and right amygdala. Coactivation patterns of individual clusters were initially revealed by meta-analytic connectivity modeling (MACM; Supporting Information Fig. S1). Functional connectivity specific to a given clusters was then determined by computing the AND conjunction between the two difference analyses of coactivation maps with the respective two other clusters. The extent threshold was set to $k = 10$ voxels. Coordinates in MNI space. **leLB**: The left cluster identified as latero-basal nuclei group was selectively coactivated with the precuneus, inferior occipital gyrus, cerebellum, superior temporal gyrus/associative auditory cortex, and middle frontal gyrus/frontal eye field on the left side, as well as bilateral temporal pole and right inferior parietal cortex. **riLB**: The right cluster identified as laterobasal nuclei group was selectively coactivated with the dorsomedial prefrontal cortex, temporal pole, precuneus, and inferior parietal cortex bilaterally, as well as the ventromedial prefrontal cortex, superior temporal gyrus/associative auditory cortex, middle frontal gyrus/frontal eye field, hippocam-pus, and posterior superior temporal sulcus on the left side. **leCM**: The left cluster identified as centromedial nuclei group was connected to the supplementary motor cortex (BA 6), pallidum, putamen, cerebellum, insula, and thalamus bilaterally (activity in right pallidum/putamen and bilateral cerebellum not depicted), as well as left posterior mid-cingulate cortex, left primary somatosensory cortex (BA 3), and right occipital lobe (V5). **riCM**: The right cluster identified as centromedial nuclei group was connected to the primary motor cortex (BA 4), supplementary motor cortex (BA 6), pallidum, putamen, primary somatosensory cortex (BA3), and inferior frontal gyrus bilaterally, as well as the right thalamus and left insula. **leSF**: The left cluster identified as superficial nuclei group was selectively coactivated with the ventral striatum/nucleus accumbens and olfactory tubercle bilaterally, as well as with the right anterior insula. **riSF:** The right cluster identified as superficial nuclei group was selectively connected to the left anterior mid-cingulate cortex and bilateral anterior insula, extending into the inferior frontal gyrus.
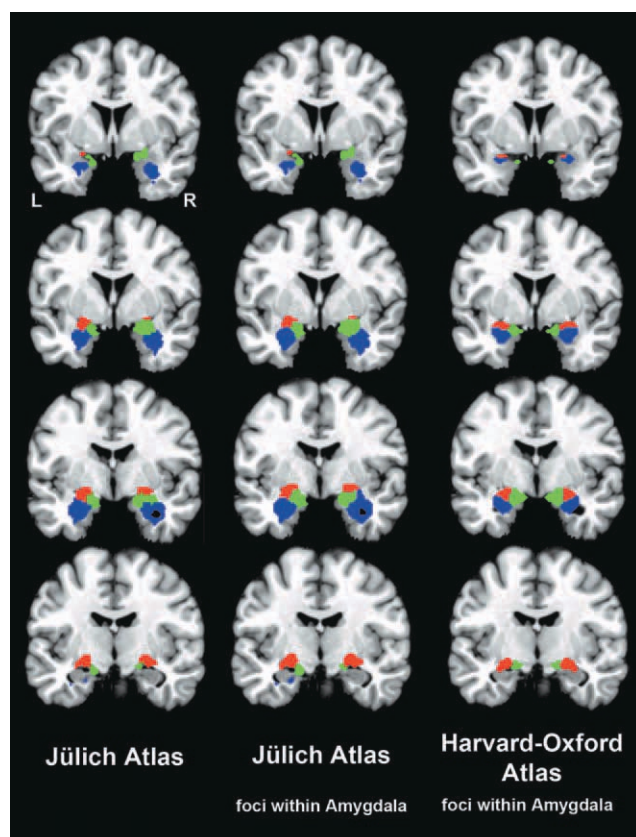
Figure 6.

Comparing different approaches to parcellating the amygdala. The left column shows coronal slices depicting the amygdala parcellation based on the maximum probability map (MPM) from the Jülich atlas using BrainMap experiments activating closest to given seed voxels without further constraints (cf. Method section). The middle column shows slices depicting a supplementary analysis based on the Jülich amygdala MPM, in which only Brain-Map experiments that activated within the histologically identified anygdala were considered for the computation of the voxel-wise coactivation patterns. The observation that 92% of all seed-voxels were assigned to corresponding clusters strongly argues against the possibility that clustering was driven by surrounding nonamygdalar activation. The right column illustrates a second supplementary analysis, in which the amygdala parcellation was based on the spatially more confined MPM from the macroanatomical Harvard–Oxford atlas. For this analysis, we again constrained the computation of coactivation patterns to BrainMap experiments that activated within the amygdala to exclude influences of adjacent regions on the coactivation patterns and hence the connectivity-based parcellation. The two confirmatory analyses provide converging evidence and hence support for the robustness of the original analysis by revealing a very similar parcellation scheme based on a more conservative CBP implementation and in an independent seed region. Blue = laterobasal nuclei group, red = centromedial nuclei group, green = superficial nuclei group.

additional parcellations, these corroborative analyses demonstrated the high robustness of the clusters' connectivity profiles even when restricting the analysis to foci located actually within the histologically identified amygdala.

Functional Characterization of the Connectivity-Derived Clusters

After assessment of the structural organization and functional connectivity, we also performed a functional characterization of the connectivity-derived clusters relying on the meta-data stored in BrainMap. All three clusters were associated with emotion and, in particular, fear processing (Fig. 7). Furthermore, the centromedial and superficial nuclei groups were linked to the emotions happiness and anger. In addition to these basic emotions, disgust was also associated with SF. Consequently, this nuclei group was significantly related to most different types of basic emotions. Consistently, all three nuclei groups were associated with observing and discriminating faces as well as passively viewing visual stimuli (Fig. 7). While only LB was linked to remembering presented items, only SF was related to passively smelling and discriminating odor. In sum, all nuclei groups were associated with emotion and viewing faces. Yet, LB was exclusively related to memory operations and SF was exclusively related to olfactory perception. Regarding the content of stimulus material presented in the databased experiments associated with the respective clusters, all three nuclei groups were associated with the presentation of faces and pictures (Supporting Information Figs. S3–S5). Moreover, the superficial nuclei group was exclusively related to olfactory stimuli. This corroborates the nuclei groups' relation with processing faces and pictures as well as SF's involvement in olfaction.

DISCUSSION

By mining neuroimaging data archived in the BrainMap database [Fox and Lancaster, 2002; Laird et al., 2005], this article demonstrates a noninvasive parcellation of the human amygdala into three clusters by task-based coactivation profiles. The shape of these clusters was in very good concordance with the earlier cytoarchitectonic segmentation into laterobasal (LB), centromedial (CM), and superficial (SF) nuclei groups [Amunts et al., 2005]. The coactivation derived clusters were subsequently characterized by the respective brain-wide functional connectivity patters and functional meta-data. Our results identify the laterobasal and centromedial nuclei groups of the human amygdala as hubs for sensory input processing and response preparation, respectively. Furthermore, the superficial nuclei group was linked to the processing of olfaction. We thus present a set of neuroinformatic methods to conjointly access structural, connectional, and functional properties of the amygdala in humans.
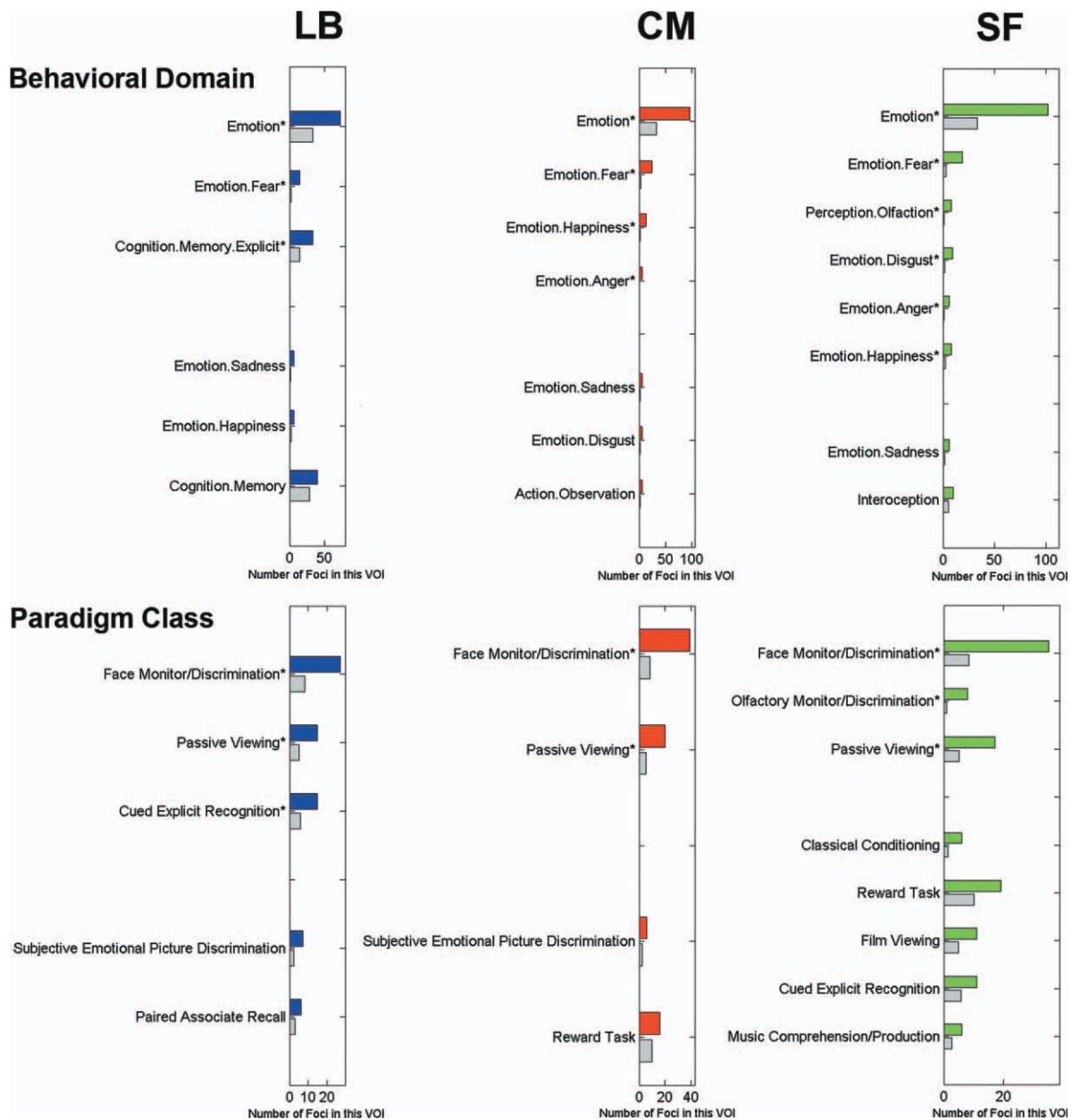
Figure 7.

Meta-data profiling of the derived clusters. Functional characterization by behavioral domain (BD) and paradigm class (PC) metadata. The colored bars denote the number of foci for the particular BD/PC within the respective derived cluster. The gray bars represent the number of foci that would be expected to hit the particular cluster if all foci with the respective BD/PC were randomly distributed throughout gray-matter. That is, the gray bars indicate the by-chance frequency of that particular label given the size of the clusters. LB = laterobasal nuclei group, CM = centromedial nuclei group, SF = superficial nuclei group. Asterisk indicates significant overrepresentation after Bonferroni correction for multiple comparisons.

Methodological Considerations of Connectivity-Based Parcellation Based on MACM

It is widely assumed that microanatomical and connectional properties constrain the brain's functional compartments [Campbell, 1905; Felleman and Van Essen, 1991; Passingham et al., 2002]. This notion has prompted the development of connectivity-based parcellation approaches. Instead of assessing the connectivity of a particular seed or within a predefined network, such algorithms aim at

delineating connectional heterogeneity within a given volume of interest. Connectivity-based parcellation has previously been performed based on DTI [Johansen-Berg et al., 2004], resting state data [Kim et al., 2010], and meta-analytic connectivity modelling [MACM; Eickhoff et al., 2011]. Here, we used the latter approach to functional connectivity analysis, which is based on assessing the brain-wide coactivation patterns of each individual seed voxel across a large number of databased neuroimaging results [Robinson et al., 2010]. It thus allows the mapping of cortical modules in a data-driven fashion based on task-based coactivation patterns.

Our analysis provided evidence for three distinct clusters with different connectivity patterns within the human amygdala. Importantly, these connectivity-derived clusters were in very good agreement with the histological subregions of the amygdala complex identified by cytoarchitectonic mapping [Amunts et al., 2005], in spite of this small region's structural and functional complexity. More specifically, the three clusters identified by MACM-based parcellation match the cytoarchitectonic definitions of the laterobasal, centromedian, and superficial nuclei with an average overlap of ~80%. The current data-driven compartmentalization thus indicated that coactivation information alone may recover microstructural heterogeneity, pointing to a close match between structure and connectivity in the human amygdala [cf. Ball et al., 2007]. From another perspective, this correspondence with microscopic boundaries further supports the biological validity of the current in vivo division of the amygdala by connectional heterogeneity.

The unveiled structural and connectional heterogeneity within the amygdala was then complemented by its functional profiling using BrainMap meta-data [Fox et al., 2005]. This indicated differences in functional response properties as discussed individually for each cluster below. The employed approach thus enabled us to link regional structural and connectional characteristics to hypotheses about functional properties. This possibility may be considered an advantage of MACM-based parcellation over parcellation techniques based on task-independent DTI or resting state data. The current approach thus employed a set of neuroinformatic methods for large-scale data mining that is potentially capable of detailing the three putative major constraints of brain organization: structure (by probabilistic histological mapping), connectivity (by coactivation mapping), and function (by meta-data profiling). The present work might thus be the first to provide direct evidence that structural, connectional, and functional characteristics reflect three different viewpoints on the same heterogeneity of a particular brain region [Passingham et al., 2002]. In light of this, connectivity-based parcellation informed by MACM might serve as a useful tool to generate hypotheses for targeted experiments assessing structural, connectional, or functional properties and their disturbances [Eickhoff et al., 2011].

Laterobasal Nuclei Group

The laterobasal amygdala is conceptualized as a likely integrator of preprocessed visual, auditory, gustatory, somatosensory, and, in part, olfactory environmental information. This is suggested by this nuclei group's connectivity profile as revealed by axonal tracing in monkeys [Aggleton et al., 1980; Iwai and Yukie, 1987; Stefanacci and Amaral, 2002; Yukie, 2002b] and by probabilistic tractography in humans [Bach et al., 2011]. Conversely, LB projects back onto sensory cortical systems in monkeys [Amaral and Price, 1984], which probably permits influencing sensory processing [Pessoa, 2010]. Indeed, links of LB with the visual cortices in monkeys [Iwai and Yukie, 1987] resonate with the inferior occipital gyrus's (IOG) exclusive connection to LB in our study. LB is further believed to represent stimulus-value associations that depend on the above-mentioned integration of perceptual input. Such stimulus-value associations could, in turn, serve as a prerequisite for various other LB-linked cognitive functions, including Pavlovian learning [Baxter and Murray, 2002], reward expectation [Pessoa, 2010], cost/benefit decisions [Ghods-Sharifi et al., 2009] and delay-discounting [Winstanley et al., 2004]. Consistent with the proposed role in coordinating higher-level sensory input, the laterobasal nuclei group was found to coactivate with the associative auditory cortex (AAC), inferior occipital gyrus, posterior superior temporal sulcus, frontal eye field, precuneus (PC), and hippocampus. Moreover, these brain regions also correlated with LB in a cytoarchitectonically informed resting state analysis [Roy et al., 2009]. Finally, a recent MACM study of the entire amygdala also revealed connectivity to these areas, except for the AAC and IOG [Robinson et al., 2010].

Importance for higher-level input processing was also accredited to the ventromedial prefrontal cortex (vmPFC) and temporal pole (TP) [Brothers, 1990; Kling and Steklis, 1976], which also coactivated with LB in the present study. In particular, the vmPFC is believed to encode learned stimulus-value relations and update reward contingencies [Kellermann et al., 2011; Kringelbach and Rolls, 2004], while TP is recognized to harbor poly-modal association areas [McDonald, 1998; Olson et al., 2007]. Our results are furthermore corroborated by the demonstration of direct connections of LB with the vmPFC and associative areas in the TP in monkeys [Aggleton et al., 1980; Ghashghaei and Barbas, 2002]. A role of the TP in higher-order input processing is further supported by similar behavioral changes in monkeys after selective amygdalectomy versus selective destruction of the temporal pole sparing the amygdala [Aggleton and Passingham, 1981; Zola-Morgan et al., 1991].

The preprocessed sensory information might be integrated with on-going thought, suggested by the functional connectivity of LB with a network comprising the medial prefrontal, inferior parietal cortices, and PC [Buckner et al., 2008]. This network has repeatedly been implicated

in self-focused reflection [Andrews-Hanna et al., 2010; Schilbach et al., 2012], mental navigation of the body in space [Maguire et al., 1997], and envisioning detached situations [Addis et al., 2009; Bzdok et al., 2012; Spreng et al., 2009]. Indeed, reflection of self-related abstract situations was argued to be an integral part of cost/benefit decisions and delay discounting [Boyer, 2008], which were both associated with LB in rats [Ghods-Sharifi et al., 2009; Winstanley et al., 2004]. Additionally, this type of hypothetical decision making might be influenced by past experience given amygdala-hippocampal connections in monkeys [Saunders et al., 1988] as well as our connectivity and function analyses of LB. We would thus conclude that the human laterobasal nuclei group may be implicated in associative processing of environmental information and the integration with self-relevant cognition. In this way, LB might subserve significance detection and associative learning processes.

Centromedial Nuclei Group

The laterobasal nuclei group is believed to send its highly preprocessed information mostly towards the centromedial group, the amygdala's putative major output center [Pitkanen et al., 1997; Solano-Castiella et al., 2010]. Integration of information originating from various intra-amygdalar circuits in the CM is likely to mediate behavioral and autonomic responses [Pessoa, 2010] as well as to facilitate attention to salient environmental cues [Barbour et al., 2010; Kapp et al., 1994]. This accords well with the observation of specific coactivation of the CM with the posterior mid-cingulate cortex (pMCC), primary motor cortex, supplementary motor area, basal ganglia, primary somatosensory cortex, insula, and thalamus. This specific connectivity, including many motor-related areas, is in line with previous data on resting state connectivity of the CM group [Roy et al., 2009] and the MACM study of the entire amygdala [Robinson et al., 2010], except for absent coactivation in the basal ganglia in the latter. Together, these results provide strong evidence that links CM to motor behavior and response preparation in humans.

Consistently, tracing studies in monkeys suggested a specific neural link from CM to the basal ganglia [Aggleton et al., 1980] and the pMCC [Morecraft et al., 2007], which corroborates our data. In fact, the pMCC is known to be implicated in response selection and skeletomotor orientation depending on reward value of behavioral outcomes [Bush et al., 2002; Shima et al., 1991]. This brain area, in turn, was reported to be connected to the primary and supplementary motor cortices in monkeys [Morecraft and Van Hoesen, 1992; Wang et al., 2001], both selectively coactivated with CM in the present study. These connectivity patters might reflect amygdalar influences on complex motor function, such as startle responses, gaze movement, and flight reaction. Please note that this potential affective-motor pathway might also mediate respond-

ent emotional facial movements [cf. Schilbach et al., 2008], which would be supported by tracer injections into the pMCC that stained both the amygdala and the facial nucleus in monkeys [Morecraft et al., 1996].

Not only motor responses but also autonomic responses have been related to CM. In particular, the CM and insula might be functionally and anatomically associated given the demonstrated coactivation and observed anatomical connections in monkeys [McDonald et al., 1996; Stefanacci and Amaral, 2002]. Notwithstanding its functional heterogeneity [Kurth et al., 2010], a major role of the insula pertains to autonomic arousal regulation, interoceptive awareness, and subjective feeling [Craig, 2002]. The likely relationship between the CM and insula might therefore consolidate the notion that CM can affect autonomic brain systems.

Almost any incoming information is channeled through the thalamus before reaching the cortex [Behrens et al., 2003; Jones, 2007]. Consequently, CM, due to connections with various thalamic regions, especially the mediodorsal (MD) nucleus, is probably able to selectively amplify and dampen early sensory input to shape environmental perception [Hunter et al., 2010]. Our findings are in support of amygdala-thalamic connections in humans that were also observed in rats [Reardon and Mitrofanis, 2000; Yasui et al., 1991] and monkeys [Aggleton and Mishkin, 1984]. We conclude that the human centromedial nuclei group might be devoted to influencing motor movement, visceral responses, and attentional reallocation.

Superficial Nuclei Group

The superficial nuclei group is thought to be involved in intraspecies communication via olfaction in nonprimate animals [Moreno and Gonzalez, 2007]. In fact, in mammals, such as rat, opossum, and rabbit, olfactory inputs mostly reach the amygdala by the superficial rather than laterobasal nuclei group [Scalia and Winans, 1975]. The exclusive association of SF with olfaction revealed in humans by the meta-data analysis and selective coactivation with the olfactory tubercle underlines a similar role of SF in human olfaction. The idea appears to be supported by projections that probably link the human SF with the olfactory Jacobson organ [Kevetter and Winans, 1981] essential to pheromone chemoreception. Pheromones, olfaction, and thus perhaps also SF, are believed to play a decisive role in social interaction, such as for social hierarchy assessment and reproductive behavior, in most mammals and probably higher primates [Dulac and Torello, 2003; Romero et al., 1990; Winans and Scalia, 1970]. Also in humans, mood [Jacob and McClintock, 2000] and sexual behavior [Cutler et al., 1998] were for instance found to be unconsciously influenced by olfactory signals. Based on the current data, we would tentatively argue that such effects may be primarily mediated by the superficial nuclei of the amygdala.

Several further lines of evidence suggest that SF is highly tuned to social information. Importantly, meta-data profiling identified SF among the three nuclei groups as significantly associated with most different basic emotions, which suggests special importance for information gleaned from human environments. Indeed, fMRI studies located highly specific responses to static [Goossens et al., 2009] and dynamic [Hurlemann et al., 2008] visual stimuli of facial emotional expressions to the human SF. Additionally, perceiving socially salient information in faces was related to activation in the anterior insula and inferior frontal gyrus [Carr et al., 2003; Wicker et al., 2003], both of which were shown to be functionally connected with SF in the present study. More broadly, prosocial value orientation was related to the superficial nuclei group in another fMRI study [Haruno and Frith, 2010]. Similarly, the size of the superficial-laterobasal amygdala complex was linked to social network size according to comparative neuroanatomical studies in non-human primates [Aggleton, 2000]. Hence, the conjunction of earlier and present findings might, indeed, advocate SF as intimately related to processing socially important input, including olfactory and emotional stimuli.

The tentative association of SF with processing socially relevant information might be further supported by the observed coactivation between SF and the nucleus accumbens. In fact, both these brain areas were previously shown to be anatomically connected in rats [Ubeda-Banon et al., 2007] and functionally connected in humans by resting-state [Roy et al., 2009] and meta-analytic connectivity modeling [Cauda et al., 2011]. Consistently, a quantitative meta-analysis on complex social judgments of faces converged exclusively in SF and the nucleus accumbens [Bzdok et al., 2011]. Furthermore, reward mechanisms, functionally subserved by the nucleus accumbens, were related to SF according to meta-data. The nucleus accumbens may therefore not only modulate approach-avoidance behavior towards basic survival needs but also towards salient social cues in human interaction [Kampe et al., 2001; Schilbach et al., 2010]. Furthermore, SF was observed to be connected with the anterior mid-cingulate cortex in the present and an earlier [Roy et al., 2009] functional connectivity analysis. As fear and pain networks overlap in the anterior mid-cingulate cortex [Vogt, 2005], it might be involved in avoidant behavior, similar to the nucleus accumbens. We conclude that the human superficial nuclei group is probably linked to olfactory, socially relevant, and reward-related processing which might functionally converge in the modulation of approach-avoidance behavior in social interaction.

Methodological Limitations

It is a wide-spread convention to question the feasibility of studying intra-amygdalar functional dissociations in humans by means of neuroimaging methods [cf. Ball et al.,

2007; Merboldt et al., 2001; Solano-Castiella et al., 2010]. In particular, it is often stressed that the processing of neuroimaging data imposes a voxel unit of roughly 4mm or larger and implies a smoothing procedure that further blurs the already rough spatial information. Smoothing indeed blurs the 3D shape of the activation signal but not the location of its activation peak. Activation peaks, however, provide the very basis for ALE meta-analysis and thus for the here presented MACM-based clustering approach of the amygdala. Apart from this theoretical consideration, we empirically refute the concern of insufficient spatial resolution by showing the topographical congruency between the neuroimaging-data-derived and the cytoarchitectonically derived subregions of the amygdala. Hence, we here formally demonstrated that the spatial resolution reached by common neuroimaging protocols permits delineating functional compartments within brain structures as tiny as the human amygdala.

On a different note, it might be objected that considering databased studies activating close to, rather than directly at, a given seed voxel might result in confounds with neighboring brain areas when computing whole-brain connectivity profiles. Yet, computing an impartial meta-analysis across dozens of studies associated with a given seed voxel entails focussing on highly conserved coactivation patterns and disfavoring spurious contributions of distant selected studies. Additionally, we applied a rather conservative cluster-level correction to the discussed connectivity map of each subregion. Moreover, it is obvious that some activation peaks, associated with individual seed voxels, might lie outside the actual seed region. Importantly, however, also considering studies activating in the immediate vicinity of the seed region acknowledges both the spatial uncertainty associated with any activation focus [Turkeltaub et al., 2002] and the inter-individual anatomical variability [Amunts et al., 2005; Robinson et al., 2010]. Taken together, connectional heterogeneity within the human amygdala was measured successfully by meta-analysis across those BrainMap studies that activate close to individual seed voxels.

CONCLUSION

We here applied connectivity-based parcellation to the human amygdala using a model-free analysis of coactivation patterns across neuroimaging studies, which was consistent with previous cytoarchitectonic reports. Combining connectivity-based parcellation, meta-analytic connectivity modeling, and meta-data profiling allowed the conjoint investigation of structural, connectional, and functional properties of the human amygdala on a subregional scale. The present findings support the laterobasal nuclei group as important for processing and integrating environmental information. The centromedial nuclei group, in turn, appeared to be implicated in mounting appropriate attentional, vegetative, and motor responses. Our results further

characterized the somewhat neglected superficial nuclei group as highly tuned to olfactory and social information processing. Ultimately, structural, connectional, and functional subspecialization concurred in the human amygdala.

REFERENCES

Adamec RE, Morgan HD (1994): The effect of kindling of different nuclei in the left and right amygdala on anxiety in the rat. Physiol Behav 55:1–12.

Addis DR, Pan L, Vu MA, Laiser N, Schacter DL (2009): Constructive episodic simulation of the future and the past: Distinct subsystems of a core brain network mediate imagining and remembering. Neuropsychologia 47:2222–2238.

Adolphs R (2008): Fear, faces, and the human amygdala. Curr Opin Neurobiol 18:166–172.

Adolphs R (2010): What does the amygdala contribute to social cognition?Ann N Y Acad Sci 1191:42–61.

Aggleton JP (2000): The Amygdala: A Functional Analysis. New York: Oxford University Press.

Aggleton JP, Burton MJ, Passingham RE (1980): Cortical and subcortical afferents to the amygdala of the rhesus monkey (*Macaca mulatta*). Brain Res 190:347–368.

Aggleton JP, Mishkin M (1984): Projections of the amygdala to the thalamus in the cynomolgus monkey. J Comp Neurol 222:56–68.

Aggleton JP, Passingham RE (1981): Syndrome produced by lesions of the amygdala in monkeys (*Macaca mulatta*). J Comp Physiol Psychol 95:961–977.

Amaral DG, Price JL (1984): Amygdalo-cortical projections in the monkey (*Macaca fascicularis*). J Comp Neurol 230:465–496.

Amaral DG, Price JL, Pitkanen A, Carmichael T (1992): Anatomical organization of the primate amygaloid complex. In: Aggleton JP, editor. The Amygdala: Neurobiological Aspects of Emotion, Memory, and Mental Dysfunction. New York: Wiley-Liss. p 1–66.

Amunts K, Kedo O, Kindler M, Pieperhoff P, Mohlberg H, Shah NJ, Habel U, Schneider F, Zilles K. (2005): Cytoarchitectonic mapping of the human amygdala, hippocampal region and entorhinal cortex: Intersubject variability and probability maps. Anat Embryol (Berl) 210:343–352.

Andrews-Hanna JR, Reidler JS, Sepulcre J, Poulin R, Buckner RL (2010): Functional-anatomic fractionation of the brain's default network. Neuron 65:550–562.

Bach DR, Behrens TE, Garrido L, Weiskopf N, Dolan RJ (2011): Deep and superficial amygdala nuclei projections revealed in vivo by probabilistic tractography. J Neurosci 31:618–623.

Ball T, Rahm B, Eickhoff SB, Schulze-Bonhage A, Speck O, Mutschler I (2007): Response properties of human amygdala subregions: Evidence based on functional MRI combined with probabilistic anatomical maps. PLoS One 2:e307.

Barbour T, Murphy E, Pruitt P, Eickhoff SB, Keshavan MS, Rajan U, Zajac-Benitez C, Diwadkar VA (2010): Reduced intra-amygdala activity to positively valenced faces in adolescent schizophrenia offspring. Schizophr Res 123:126–136.

Baxter MG, Murray EA (2002): The amygdala and reward. Nat Rev Neurosci 3:563–573.

Behrens TE, Johansen-Berg H, Woolrich MW, Smith SM, Wheeler-Kingshott CA, Boulby PA, Barker GJ, Sillery EL, Sheehan K, Ciccarelli O, Thompson AJ, Brady JM, Matthews PM (2003): Non-invasive mapping of connections between human thalamus and cortex using diffusion imaging. Nat Neurosci 6:750–757.

Boyer P (2008): Evolutionary economics of mental time travel?-Trends Cogn Sci 12:219–224.

Brothers L (1990): The social brain: A project for integrating primate behavior and neurophysiology in a new domain. Concepts Neurosci 1:27–51.

Buckner RL, Andrews-Hanna JR, Schacter DL (2008): The brain's default network: Anatomy, function, and relevance to disease. Ann N Y Acad Sci 1124:1–38.

Bush G, Vogt BA, Holmes J, Dale AM, Greve D, Jenike MA, Rosen BR (2002): Dorsal anterior cingulate cortex: A role in reward-based decision making. Proc Natl Acad Sci USA 99:523–528.

Bzdok D, Langner R, Caspers S, Kurth F, Habel U, Zilles K, Laird A, Eickhoff SB (2011): ALE meta-analysis on facial judgments of trustworthiness and attractiveness. Brain Struct Funct 215:209–223.

Bzdok D, Langner R, Hoffstaedter F, Turetsky B, Zilles K, Eickhoff SB (2012): The modular neuroarchitecture of social judgments on faces. Cereb Cortex 22:951–961.

Bzdok D, Schilbach L, Vogeley K, Schneider K, Laird AR, Langner R, Eickhoff SB:Parsing the neural correlates of moral cognition: ALE meta-analysis on morality, theory of mind, and empathy. Brain Struct Funct (in press).

Campbell AW (1905): Histological Studies on the Localisation of Cerebral Function. Cambridge, UK: Cambridge University Press.

Carr L, Iacoboni M, Dubeau MC, Mazziotta JC, Lenzi GL (2003): Neural mechanisms of empathy in humans: A relay from neural systems for imitation to limbic areas. Proc Natl Acad Sci USA 100:5497–5502.

Cauda F, Cavanna AE, D'Agata F, Sacco K, Duca S, Geminiani GC (2011): Functional connectivity and coactivation of the nucleus accumbens: A combined functional connectivity and structure-based meta-analysis. J Cogn Neurosci 23:2864–2877.

Craig AD (2002): How do you feel? Interoception: The sense of the physiological condition of the body. Nat Rev Neurosci 3:655–666.

Cutler WB, Friedmann E, McCoy NL (1998): Pheromonal influences on sociosexual behavior in men. Arch Sex Behav 27:1–13.

Davis M, Whalen PJ (2001): The amygdala: Vigilance and emotion. Mol Psychiatry 6:13–34.

Dulac C, Torello AT (2003): Molecular detection of pheromone signals in mammals: From genes to behaviour. Nat Rev Neurosci 4:551–562.

Eickhoff SB, Bzdok D (2012): Database-driven identification of functional modules in the cerebral cortex. In: Geyer S, Turner R, editors. Microstructural Parcellation of the Human Cerebral Cortex. Heidelberg: Springer.

Eickhoff SB, Bzdok D: Meta-analyses in basic and clinical neuroscience: State of the art and perspective. In: Ulmer S, Jansen O, editors. fMRI—Basics and Clinical Applications, 2nd ed. Heidelberg: Springer.

Eickhoff SB, Stephan KE, Mohlberg H, Grefkes C, Fink GR, Amunts K, Zilles K (2005): A new SPM toolbox for combining probabilistic cytoarchitectonic maps and functional imaging data. Neuroimage 25:1325–1335.

Eickhoff SB, Heim S, Zilles K, Amunts K (2006): Testing anatomically specified hypotheses in functional imaging using cytoarchitectonic maps. Neuroimage 32:570–582.

Eickhoff SB, Rottschy C, Zilles K (2007): Laminar distribution and co-distribution of neurotransmitter receptors in early human visual cortex. Brain Struct Funct 212:255–267.

Eickhoff SB, Laird AR, Grefkes C, Wang LE, Zilles K, Fox PT (2009): Coordinate-based activation likelihood estimation meta-analysis of neuroimaging data: A random-effects approach based on empirical estimates of spatial uncertainty. Hum Brain Mapp 30:2907–2926.

Eickhoff SB, Bzdok D, Laird AR, Roski C, Caspers S, Zilles K, Fox PT (2011): Co-activation patterns distinguish cortical modules, their connectivity and functional differentiation. Neuroimage 57:938–949.

Eickhoff SB, Bzdok D, Laird AR, Kurth F, Fox PT (2012): Activation likelihood estimation meta-analysis revisited. Neuroimage 59:2349–2361.

Felleman DJ, Van Essen DC (1991): Distributed hierarchical processing in the primate cerebral cortex. Cereb Cortex 1:1–47.

Fox PT, Lancaster JL (2002): Opinion: Mapping context and content: The BrainMap model. Nat Rev Neurosci 3:319–321.

Fox PT, Laird AR, Fox SP, Fox PM, Uecker AM, Crank M, Koenig SF, Lancaster JL (2005): BrainMap taxonomy of experimental design: Description and evaluation. Hum Brain Mapp 25:185–198.

Friston KJ, Frith CD, Fletcher P, Liddle PF, Frackowiak RS (1996): Functional topography: Multidimensional scaling and functional connectivity in the brain. Cereb Cortex 6:156–164.

Fudge JL, Haber SN (2000): The central nucleus of the amygdala projection to dopamine subpopulations in primates. Neuroscience 97:479–494.

Ghashghaei HT, Barbas H (2002): Pathways for emotion: Interactions of prefrontal and anterior temporal pathways in the amygdala of the rhesus monkey. Neuroscience 115:1261–1279.

Ghods-Sharifi S, St Onge JR, Floresco SB (2009): Fundamental contribution by the basolateral amygdala to different forms of decision making. J Neurosci 29:5251–5259.

Goossens L, Kukolja J, Onur OA, Fink GR, Maier W, Griez E, Schruers K, Hurlemann R (2009): Selective processing of social stimuli in the superficial amygdala. Hum Brain Mapp 30:3332–3338.

Hall E (1972): Some aspects of the structural organization of the amygdala. In: Eleftheriou BE, editor. The Neurobiology of the Amygdala. New York: Plenum. p 95–122.

Hardee JE, Thompson JC, Puce A (2008): The left amygdala knows fear: Laterality in the amygdala response to fearful eyes. Soc Cogn Affect Neurosci 3:47–54.

Hartigan JA, Wong MA (1979): A k-means clustering algorithm. Appl Stat 28:100–108.

Haruno M, Frith CD (2010): Activity in the amygdala elicited by unfair divisions predicts social value orientation. Nat Neurosci 13:160–161.

Heimer L, Van Hoesen GW (2006): The limbic lobe and its output channels: Implications for emotional functions and adaptive behavior. Neurosci Biobehav Rev 30:126–147.

Hunter MD, Eickhoff SB, Pheasant RJ, Douglas MJ, Watts GR, Farrow TF, Hyland D, Kang J, Wilkinson ID, Horoshenkov KV, Woodruff PW (2010): The state of tranquility: Subjective perception is shaped by contextual modulation of auditory connectivity. Neuroimage 53:611–618.

Hurlemann R, Rehme AK, Diessel M, Kukolja J, Maier W, Walter H, Cohen MX (2008): Segregating intra-amygdalar responses to dynamic facial emotion with cytoarchitectonic maximum probability maps. J Neurosci Methods 172:13–20.

Iwai E, Yukie M (1987): Amygdalofugal and amygdalopetal connections with modality-specific visual cortical areas in maca-ques (*Macaca fuscata*, *M. mulatta*, and *M. fascicularis*). J Comp Neurol 261:362–387.

Jacob S, McClintock MK (2000): Psychological state and mood effects of steroidal chemosignals in women and men. Horm Behav 37:57–78.

Johansen-Berg H, Behrens TE, Robson MD, Drobnjak I, Rushworth MF, Brady JM, Smith SM, Higham DJ, Matthews PM (2004): Changes in connectivity profiles define functionally distinct regions in human medial frontal cortex. Proc Natl Acad Sci USA 101:13335–13340.

Jones EG (2007): The Thalamus. Cambridge: Cambridge University Press.

Kampe KK, Frith CD, Dolan RJ, Frith U (2001): Reward value of attractiveness and gaze. Nature 413:589.

Kapp BS, Supple WF Jr, Whalen PJ (1994): Effects of electrical stimulation of the amygdaloid central nucleus on neocortical arousal in the rabbit. Behav Neurosci 108:81–93.

Kellermann TS, Sternkopf MA, Schneider F, Habel U, Turetsky BI, Zilles K, Eickhoff SB (2012): Modulating the processing of emotional stimuli by cognitive demand. Soc Cogn Affect Neurosci 7:263–273.

Kevetter GA, Winans SS (1981): Connections of the corticomedial amygdala in the golden hamster. I. Efferents of the "vomeronasal amygdala". J Comp Neurol 197:81–98.

Killcross S, Robbins TW, Everitt BJ (1997): Different types of fear-conditioned behaviour mediated by separate nuclei within amygdala. Nature 388:377–380.

Kim JH, Lee JM, Jo HJ, Kim SH, Lee JH, Kim ST, Seo SW, Cox RW, Na DL, Kim SI, Saad ZS (2010): Defining functional SMA and pre-SMA subregions in human MFC using resting state fMRI: Functional connectivity-based parcellation method. Neuroimage 49:2375–2386.

Kling A, Steklis HD (1976): A neural substrate for affiliative behavior in nonhuman primates. Brain Behav Evol 13:216–238.

Kringelbach ML, Rolls ET (2004): The functional neuroanatomy of the human orbitofrontal cortex: Evidence from neuroimaging and neuropsychology. Prog Neurobiol 72:341–372.

Kurth F, Zilles K, Fox PT, Laird AR, Eickhoff SB (2010): A link between the systems: Functional differentiation and integration within the human insula revealed by meta-analysis. Brain Struct Funct 214:519–534.

Laird AR, Lancaster JL, Fox PT (2005): BrainMap: The social evolution of a human brain mapping database. Neuroinformatics 3:65–78.

Laird AR, Eickhoff SB, Kurth F, Fox PM, Uecker AM, Turner JA, Robinson JL, Lancaster JL, Fox PT (2009a): ALE meta-analysis workflows via the brainmap database: Progress towards a probabilistic functional brain atlas. Front Neuroinform 3:23.

Laird AR, Eickhoff SB, Li K, Robin DA, Glahn DC, Fox PT (2009b): Investigating the functional heterogeneity of the default mode network using coordinate-based meta-analytic modeling. J Neurosci 29:14496–14505.

Laird AR, Lancaster JL, Fox PT (2009c): Lost in localization? The focus is meta-analysis. Neuroimage 48:18–20.

Laird AR, Eickhoff SB, Fox PM, Uecker AM, Ray KL, Saenz JJ Jr, McKay DR, Bzdok D, Laird RW, Robinson JL, Turner JA, Turkeltaub PE, Lancaster JL, Fox PT (2011): The brainmap strategy for standardization, sharing, and meta-analysis of neuroimaging data. BMC Res Notes 4:349.

LeDoux JE (2000): Emotion circuits in the brain. Annu Rev Neurosci 23:155–184.

LeDoux JE (2007): The amygdala. Curr Biol 17:R868–R874.

Maguire EA, Frackowiak RS, Frith CD (1997): Recalling routes around london: Activation of the right hippocampus in taxi drivers. J Neurosci 17:7103–7110.

McDonald AJ (1992): Cell types and intrinsic connections of the amygdala. In: Aggleton JP, editor. The Amygdala: Neurobiological Aspects of Emotion, Memory, and Mental Dysfunction. New York: Wiley Liss. p 67–96.

McDonald AJ (1998): Cortical pathways to the mammalian amygdala. Prog Neurobiol 55:257–332.

McDonald AJ, Mascagni F, Guo L (1996): Projections of the medial and lateral prefrontal cortices to the amygdala: A Phaseolus vulgaris leucoagglutinin study in the rat. Neuroscience 71:55–75.

Merboldt KD, Fransson P, Bruhn H, Frahm J (2001): Functional MRI of the human amygdala? Neuroimage 14:253–257.

Morecraft RJ, Van Hoesen GW (1992): Cingulate input to the primary and supplementary motor cortices in the rhesus monkey: Evidence for somatotopy in areas 24c and 23c. J Comp Neurol 322:471–489.

Morecraft RJ, Schroeder CM, Keifer J (1996): Organization of face representation in the cingulate cortex of the rhesus monkey. Neuroreport 7:1343–1348.

Morecraft RJ, McNeal DW, Stilwell-Morecraft KS, Gedney M, Ge J, Schroeder CM, van Hoesen GW (2007): Amygdala interconnections with the cingulate motor cortex in the rhesus monkey. J Comp Neurol 500:134–165.

Moreno N, Gonzalez A (2007): Evolution of the amygdaloid complex in vertebrates, with special reference to the anamnio-amniotic transition. J Anat 211:151–163.

Morris JS, Frith CD, Perrett DI, Rowland D, Young AW, Calder AJ, Dolan RJ.(1996): A differential neural response in the human amygdala to fearful and happy facial expressions. Nature 383:812–815.

Morris JS, Ohman A, Dolan RJ (1999): A subcortical pathway to the right amygdala mediating "unseen" fear. Proc Natl Acad Sci USA 96:1680–1685.

Mosher CP, Zimmerman PE, Gothard KM (2010): Response characteristics of basolateral and centromedial neurons in the primate amygdala. J Neurosci 30:16197–16207.

Müller VI, Habel U, Derntl B, Schneider F, Zilles K, Turetsky BI, Eickhoff SB (2011): Incongruence effects in crossmodal emotional integration. Neuroimage 54:2257–2266.

Nanetti L, Cerliani L, Gazzola V, Renken R, Keysers C (2009): Group analyses of connectivity-based cortical parcellation using repeated k-means clustering. Neuroimage 47:1666–1677.

Nickl-Jockschat T, Habel U, Maria Michel T, Manning J, Laird AR, Fox PT, Schneider F, Eickhoff SB (2012): Brain structure anomalies in autism spectrum disorder-a meta-analysis of VBM studies using anatomic likelihood estimation. Hum Brain Mapp 33:1470–1489.

Öhman A (2009): Of snakes and faces: An evolutionary perspective on the psychology of fear. Scand J Psychol 50:543–552.

Olson IR, Ploaker A, Ezzyat Y (2007): The Enigmatic temporal pole: A review of findings on social and emotional processing. Brain 130:1718–1731.

Ousdal OT, Jensen J, Server A, Hariri AR, Nakstad PH, Andreassen OA (2008): The human amygdala is involved in general behavioral relevance detection: Evidence from an event-related functional magnetic resonance imaging Go-NoGo task. Neuroscience 156:450–455.

Packard MG, Cahill L (2001): Affective modulation of multiple memory systems. Curr Opin Neurobiol 11:752–756.

Passingham RE, Stephan KE, Kotter R (2002): The anatomical basis of functional localization in the cortex. Nat Rev Neurosci 3:606–616.

Pessoa L (2010): Emotion and cognition and the amygdala: From "what is it?" to "what's to be done?". Neuropsychologia 48:3416–3429.

Phelps EA, LeDoux JE (2005): Contributions of the amygdala to emotion processing: From animal models to human behavior. Neuron 48:175–187.

Pitkanen A, Savander V, LeDoux JE (1997): Organization of intra-amygdaloid circuitries in the rat: An emerging framework for understanding functions of the amygdala. Trends Neurosci 20:517–523.

Poldrack RA (2006): Can cognitive processes be inferred from neuroimaging data?Trends Cogn Sci 10:59–63.

Price C, Friston K (2005): Functional ontologies for cognition: The systematic definition of structure and function. Cogn Neuropsychol 22:262–275.

Price JL, Russchen FT, Amaral DG (1987): The limbic region. II: The amygdaloid complex. In: Björklund A, Hökfelt T, Swanson LW, editors. Handbook of Chemical Neuroanatomy. Amsterdam: Elsevier. p 279–388.

Reardon F, Mitrofanis J (2000): Organisation of the amygdalo-thalamic pathways in rats. Anat Embryol (Berl) 201:75–84.

Robinson JL, Laird AR, Glahn DC, Lovallo WR, Fox PT (2010): Metaanalytic connectivity modeling: Delineating the functional connectivity of the human amygdala. Hum Brain Mapp 31:173–184.

Romero PR, Beltramino CA, Carrer HF (1990): Participation of the olfactory system in the control of approach behavior of the female rat to the male. Physiol Behav 47:685–690.

Roy AK, Shehzad Z, Margulies DS, Kelly AM, Uddin LQ, Gotimer K, Biswal BB, Castellanos FX, Milham MP (2009): Functional connectivity of the human amygdala using resting state fMRI. Neuroimage 45:614–626.

Sah P, Faber ES, Lopez De Armentia M, Power J (2003): The amygdaloid complex: Anatomy and physiology. Physiol Rev 83:803–834.

Sander D, Grafman J, Zalla T (2003): The human amygdala: An evolved system for relevance detection. Rev Neurosci 14:303–316.

Saunders RC, Rosene DL, Van Hoesen GW (1988): Comparison of the efferents of the amygdala and the hippocampal formation in the rhesus monkey: II. Reciprocal and non-reciprocal connections. J Comp Neurol 271:185–207.

Saygin ZM, Osher DE, Augustinack J, Fischl B, Gabrieli JD (2011): Connectivity-based segmentation of human amygdala nuclei using probabilistic tractography. Neuroimage 56:1353–1361.

Scalia F, Winans SS (1975): The differential projections of the olfactory bulb and accessory olfactory bulb in mammals. J Comp Neurol 161:31–55.

Schilbach L, Eickhoff SB, Mojzisch A, Vogeley K (2008): What's in a smile? Neural correlates of facial embodiment during social interaction. Soc Neurosci 3:37–50.

Schilbach L, Wilms M, Eickhoff SB, Romanzetti S, Tepest R, Bente G, Shah NJ, Fink GR, Vogeley K (2010): Minds made for sharing: Initiating joint attention recruits reward-related neurocircuitry. J Cogn Neurosci 22:2702–2715.

Schilbach L, Bzdok D, Timmermans B, Fox PT, Laird AR, Vogeley K, Eickhoff SB (2012): Introspective minds: Using ALE meta-analyses to study commonalities in the neural correlates of emotional processing, social and unconstrained cognition. PLoS One 7:e30920.

Shima K, Aya K, Mushiake H, Inase M, Aizawa H, Tanji J (1991): Two movement-related foci in the primate cingulate cortex observed in signal-triggered and self-paced forelimb movements. J Neurophysiol 65:188–202.

Smith SM, Jenkinson M, Woolrich MW, Beckmann CF, Behrens TE, Johansen-Berg H, Bannister PR, De Luca M, Drobnjak I, Flitney DE, Niazy RK, Saunders J, Vickers J, Zhang Y, De Stefano N, Brady JM, Matthews PM (2004): Advances in functional and structural MR image analysis and implementation as FSL. Neuroimage 23 (Suppl 1):S208–S219.

Solano-Castiella E, Anwander A, Lohmann G, Weiss M, Docherty C, Geyer S, Reimer E, Friederici AD, Turner R (2010): Diffusion tensor imaging segments the human amygdala in vivo. Neuroimage 49:2958–2965.

Solano-Castiella E, Schafer A, Reimer E, Turke E, Proger T, Lohmann G, Trampel R, Turner R (2011): Parcellation of human amygdala in vivo using ultra high field structural MRI. Neuroimage 58:741–748.

Spreng RN, Mar RA, Kim AS (2009): The common neural basis of autobiographical memory, prospection, navigation, theory of mind, and the default mode: A quantitative meta-analysis. J Cogn Neurosci 21:489–510.

Stefanacci L, Amaral DG (2002): Some observations on cortical inputs to the macaque monkey amygdala: An anterograde tracing study. J Comp Neurol 451:301–323.

Swanson LW, Petrovich GD (1998): What is the amygdala? Trends Neurosci 21:323–331.

Timm NH (2002): Applied Multivariate Analysis. New York: Springer.

Toga AW (2002): Imaging databases and neuroscience. Neuroscientist 8:423–436.

Turkeltaub PE, Eden GF, Jones KM, Zeffiro TA (2002): Meta-analysis of the functional neuroanatomy of single-word reading: Method and validation. Neuroimage 16:765–780.

Turkeltaub PE, Eickhoff SB, Laird AR, Fox M, Wiener M, Fox P (2012): Minimizing within-experiment and within-group effects in activation likelihood estimation meta-analyses. Hum Brain Mapp 33:1–13.

Turner BH, Mishkin M, Knapp M (1980): Organization of the amygdalopetal projections from modality-specific cortical association areas in the monkey. J Comp Neurol 191:515–543.

Ubeda-Banon I, Novejarque A, Mohedano-Moriano A, Pro-Sistiaga P, de la Rosa-Prieto C, Insausti R, Martinez-Garcia F, Lanuza E, Martinez-Marcos A (2007): Projections from the posterolateral olfactory amygdala to the ventral striatum: Neural basis for reinforcing properties of chemical stimuli. BMC Neuroscience 8:103.

Vogt BA (2005): Pain and emotion interactions in subregions of the cingulate gyrus. Nat Rev Neurosci 6:533–544.

Wang Y, Shima K, Sawamura H, Tanji J (2001): Spatial distribution of cingulate cells projecting to the primary, supplementary, and pre-supplementary motor areas: A retrograde multiple labeling study in the macaque monkey. Neurosci Res 39:39–49.

Wicker B, Keysers C, Plailly J, Royet JP, Gallese V, Rizzolatti G (2003): Both of us disgusted in My Insula: The common neural basis of seeing and feeling disgust. Neuron 40:655–664.

Winans SS, Scalia F (1970): Amygdaloid nucleus: New afferent input from the vomeronasal organ. Science 170:330–332.

Winstanley CA, Theobald DE, Cardinal RN, Robbins TW (2004): Contrasting roles of basolateral amygdala and orbitofrontal cortex in impulsive choice. J Neurosci 24:4718–4722.

Yasui Y, Saper CB, Cechetto DF (1991): Calcitonin gene-related peptide (CGRP) immunoreactive projections from the thalamus to the striatum and amygdala in the rat. J Comp Neurol 308:293–310.

Yukie M (2002a): Connections between the amygdala and auditory cortical areas in the macaque monkey. Neurosci Res 42:219–229.

Yukie M (2002b): Connections between the amygdala and auditory cortical areas in the macaque monkey. Neurosci Res 42:219–229.

Zilles K, Schleicher A, Palomero-Gallagher N, Amunts K (2002): Quantitative analysis of cyto- and receptor architecture of the human brain. In: Mazziotta JC, Toga AW, editors. Brain Mapping, the Methods. Academic, San Diego. p 573–602.

Zola-Morgan S, Squire LR, Alvarez-Royo P, Clower RP (1991): Independence of memory functions and emotional behavior: Separate contributions of the hippocampal formation and the amygdala. Hippocampus 1:207–220.